Scaling laws of density fluctuations at high-k on Tore Supra

P. Hennequin, R Sabot, C Honoré, G T Hoang, X Garbet, A Truc, C Fenzi, A Quéméneur

Scaling laws of density fluctuations at high-k on Tore Supra

P. Hennequin†, R. Sabot‡, C. Honoré†, G.T. Hoang‡, X. Garbet‡, A. Truc†, C. Fenzi‡, A. Quéméneur†.

† Laboratoire de Physique et Technologie des Plasmas,
CNRS-Ecole Polytechnique, 91128 Palaiseau cedex, France
‡ Association Euratom-CEA , CEA/DSM/DRFC, Centre de Cadarache,
13108 St Paul lèz Durance, France

Abstract. Anomalous transport in tokamaks is generally attributed to turbulent fluctuations. Since a large variety of modes are potentially unstable, a wide range of short-scale fluctuations should be measured, with wavenumbers from $k\rho_i \sim 0.1$ to $k\rho_i >> 1$. On the Tore Supra tokamak, a light scattering experiment has made possible fluctuation measurements in the medium and high-k domains where a transition in the k-spectrum is observed: The fluctuation level decreases much faster than usual observations, typically with a power law $S(k) \equiv k^{-6}$. A scan of the ion Larmor radius shows that the transition wavenumber scales with ρ_i around $k\rho_i \sim 1.5$. This transition indicates that a characteristic length scale should be involved to describe the fluctuation non linear dynamics in this range. The resulting very low level of fluctuations at high k does not support a strong effect of turbulence driven by electron temperature gradient. For this gyroradius scan, the characteristics of turbulence also exhibit a good matching with predictions from gyro-Bohm scaling: the typical scale length of turbulence scales with the ion Larmor radius, the typical time scales with a/c_s; the turbulence level also scales with ρ_i, according to the mixing length rule.

Submitted to: *Plasma Phys. Control. Fusion*

1. Introduction

The problem of anomalous transport of energy and particles across magnetic surfaces in fusion devices has raised a considerable interest for long. This is an important issue for a reactor since transport determines the quality of confinement in a magnetized fusion plasma. The large transport coefficients, much larger than neoclassical values, are attributed to turbulence driven by temperature and density gradients [1, 2]. Though significant progress has been made [3], the underlying instabilities are still a subject of debate. Indeed, a large variety of modes can become unstable, and they differ in particular by their typical scale (e. g. their correlation length or equivalently the inverse of their wavenumber $1/k_\perp$). The most commonly invoked [4] are the ion temperature gradient mode (ITG) with a typical scale longer than the ion Larmor radius ρ_i ($k_\perp \rho_i <\sim 1$), the trapped electron mode (TEM) also of the order of ρ_i, and the smaller scale electron temperature gradient mode (ETG), with $k_\perp \rho_i >> 1$. The turbulence at the largest scale (ITG, TEM) is believed to be responsible for the most part of transport; this is consistent with fluctuations observed in tokamaks [5, 6, 7, 8, 9] which are mainly distributed in the range $k_\perp \rho_i$ from 0.1 to 0.5, and strongly correlated with the high level of anomalous transport.

However, in high confinement regimes associated with the formation of transport barrier such as Internal Transport Barrier discharges, it is observed that the ion thermal transport can be reduced down to neoclassical values, accompanied by a reduction of the largest scale turbulence [10, 11], while the electron transport channel remains at a high level [12]. This could be due to fluctuations at high k linked with ETG modes. Experiments with dominant electron heating have exhibited a critical electron temperature threshold which also pointed toward the potential role of ETG modes [13, 14]. These regimes deserve attention since the alpha particles will heat mainly electrons in burning plasmas. Several theoretical and numerical studies have recently shown that ETG modes could account for a significant part of electron transport [15, 16, 17] due to the formation of long scale structures in the radial direction.

Determining how the turbulence scales with plasma typical length scales such as the Larmor radius is important not only to identify the driving mechanism, but also to provide constraints on transport models and their dependence on the global dimensionless parameters. Indeed in the absence of a fully comprehensive model for anomalous transport, the extrapolation of energy confinement and fusion performance relies on scaling laws of confinement based on a multi-machine data base. Transport coefficients, normalised to the Bohm value $\chi_B \equiv T/eB$, can be expressed as functions of three dimensionless parameters $\chi \equiv \chi_B F(\rho^*, \nu^*, \beta)$ [18, 19], where $\rho^* (\equiv \rho_i/a)$ is the normalized gyroradius, ν^* the collisionality and β the ratio of

kinetic to magnetic pressure. In these similarity analysis, the value of the parameter ρ^* expected on the next step machines is not achievable in the present experiments. The large extrapolation required for the design of the next step machine requires the determination of χ scaling with ρ^* with the highest accuracy, which could benefit from confrontation of these scaling laws to turbulent transport models and turbulence measurements. An explicite dependence $\chi \equiv \chi_B \rho^*$ (gyro-Bohm scaling), which is favorable, is observed experimentally for the electron transport channel, and the ion transport channel in High confinement regime. Numerical simulations usually predict a gyro-Bohm behaviour for small ρ^*. This implies that the typical scale length of turbulence is the Larmor gyroradius, and the correlation time of the order of the transit time a/c_s. Indeed a crude estimate of the transport diffusion coefficient can be obtained from analogy with random walk, $\chi \sim \rho^2 c_s/a \equiv \rho^* T/eB$ which leads to a gyro-Bohm scaling of the turbulent transport. Furthermore, the mixing length rule [3, 20] predicts that turbulence saturates when the convection of perturbated density balances the linear drive (convection of average density): the relative level of fluctuations is mostly observed to scale with ρ_i/L_p, where L_p is the pressure gradient length [5, 9, 21, 22]. Determining the scaling of turbulence length scales and level with the Larmor radius provides tests of these scalings. Experimental results are generally in agreement with gyro-Bohm behaviour [9, 21, 23].

A further interest for analysing fluctuations on a wide range of scales is that the distribution of fluctuation level among the scales characterizes the non linear dynamics and the energy transfer process between scales. A classical example is the Kolmogorov law in 3D isotropic fluid turbulence [24], where energy injected at large scale is redistributed by non linear interactions down to the dissipative length. This characteristic decay of large vortices breaking into smaller ones has been described by Kolmogorov in terms of an energy cascade $E(k) \equiv k^{-5/3}$ in the inertial range, where $E(k)$ is the kinetic energy at the scale $1/k$ ($\int E(k)dk = 1/2 < v^2 >$). It assumes that far from production and dissipation ranges, the energy transfer is local and independent of the scale. The situation is different in 2D fluid turbulence because in addition to energy, enstrophy is also an invariant, and a dual cascade takes place on either side of the length scale at which energy is injected [25]: the energy cascade is in that case directed towards larger scales, with the same spectral index $E(k) \equiv k^{-5/3}$, leading to the formation of large structures. The direct enstrophy cascade follows a power law $E(k) \equiv k^{-3}$ for smaller scales down to the dissipation length-scale [26]. Because of the strong anisotropy induced by the large magnetic field, turbulence perpendicular and parallel wavenumbers are very different $k_\parallel << k_\perp$; magnetised plasma turbulence is then expected to follow this 2D picture [27, 28] implying a mode condensation (formation of large scale structures) below the wavenumber k_f of the driving instability. The wavenumber k_f delimiting (at the transition between) the direct and inverse cascade spectral zones varies with the different models ($k\rho_i < 1$) [4, 28, 29]). Nevertheless tokamak plasma turbulence may depart from this simplified

description [4, 29] for different reasons: 3D effects, a larger complexity involving multi-field dynamics with different invariants, the possibility to inject energy at different scales.

The scattering of electromagnetic waves is a powerful technique for the purpose of fine scale analysis, because it provides directly the space Fourier transform of the fluctuating density at a specified wavenumber. It as been used since the early fluctuation measurements in tokamaks. It was found that the most energetic part of the wavenumber spectrum (i.e. the spectral density of fluctuations $S(\vec{k}) \equiv |n(\vec{k})^2|$ at the wavenumber $\vec{k}$) lay below $k_\perp \rho_i < 1$ [30, 31, 33]. For larger machines, a difference is observed at small $k_\perp$ between the poloidal and radial wavenumber spectra [5, 34]: a maximum around $k_\theta \rho_i \sim 0.3$ is observed in the poloidal direction, not in the radial direction. This is also observed with other density fluctuation measurements like beam emission spectroscopy [6, 8, 9], and correlation reflectometry [23]: very long correlations lengths of fluctuations are measured typically around 5 to 10 ρ_i ($k_\perp \rho_i \sim 0.1$). Above this maximum, the fluctuation wavenumber spectrum $S(k_\perp)$ falls off monotonically [32, 33], following a power law $S(k) \propto k^{-a}$. The power exponent is $a \sim 3.5 \pm 0.5$ for most experiments [5, 7, 36]. This is close to the exponent expected in the direct cascade range for the measured tri-dimensional wavenumber spectrum, i.e for $\vec{k}$ fixed in modulus and direction: for all wave numbers in the perpendicular plane having the same modulus, the omni-directional k spectrum $E(k) \equiv \int_{|\vec{k}_\perp|=k} S(\vec{k}_\perp) d\vec{k}_\perp = kS(|\vec{k}_\perp| = k)$; assuming isotropy in the perpendicular plane, a 3D spectrum with a scaling exponent of -4 yields $E(k)$ with a spectral index of -3. This exponent is generally used for practical transport coefficient estimate from fluctuation level. In 3D fluid turbulence, light scattering has also permitted to measure the k spectrum [37] indicating a very good agreement between the measured spectral index of $-3.6 \sim -11/3$, and the expected one from the Kolmogorov law $E(k) \equiv k^2 E_{3D}(\vec{k}) \equiv k^{-5/3}$.

In the Tore Supra tokamak, the CO_2 laser scattering experiment ALTAIR [38] was designed for direct and detailed study of turbulence scales, with a high wavelength resolution in the range $3 < k_\perp < 15$ cm^{-1}. Higher $k_\perp$ value, up to 26 cm^{-1} have been reached thanks to a modification in the experimental set-up. This exploration at larger k turned out to depart substantially from the usual power law, showing a transition around $k_c = 15$ cm^{-1} [39]. In this paper, after introducing the experimental set-up (§ 2), we investigate the wavenumber spectrum in Ohmic and L mode plasmas (§3), particularly the fast decrease of turbulence at high k. We show how the wavenumber value at the k spectrum transition scales with plasma parameters, especially with the ion gyroradius. This is achieved by varying the magnetic field by a factor of two, resulting in a change in the Larmor radius around 30% in the edge where fluctuations are measured. We then use this gyroradius scan for comparing the fluctuation level (§4) and correlation time (§5) scalings with expectations from a gyro-Bohm scaling.

2. Experimental setup for large k fluctuation measurements

2.1. Modification of the ALTAIR optical configuration

The ALTAIR diagnostic [38] is based on coherent forward Thomson scattering. The signal received on the detector is proportional to the spatial Fourier transform of density fluctuations at the scale corresponding to the scattering wavevector $\vec{k}$, which is the difference between the incident and scattered beam wavenumbers $\vec{k}_i - \vec{k}_d$ (Bragg selection rule):

$$i_{det}(\vec{k}, t) = \int u(\vec{r}) n(\vec{r}, t) e^{i\vec{k}\vec{r}} d^3r$$

($u(\vec{r})$ defines the scattering volume, intersection of the incident and scattered beams).

The probing beam, provided by a CO_2 laser ($\lambda = 10.6\,\mu$m) is split in 3 parts, a low amplitude Local Oscillator crossing the plasma along a vertical chord, and 2 main beams, crossing the LO beam with a small angle. The scattering angles θ can be set independently for each channel and define the scattering wavenumber modulus $k = 2k_i \sin(\theta_i/2)$. Moreover, the main beams can be rotated around the LO beam with an angle α with respect to $\vec{u}_R$ (unit vector along the major radius in the poloidal plane). The wavevector can thus be set to be perpendicular to the magnetic field $\vec{B}$ in a local area of the chord ($\vec{B}$ direction varies along the chord due to magnetic shear). The scattered wave vector is then horizontal, perpendicular to the magnetic field and has no radial component since the chord is central. The beams are also shifted by different frequencies for heterodyne detection. Several fast data acquisitions (acquisition rate 5 MHz) with long time sequence can be triggered during a shot; the RMS value of each channel signal is also recorded during the whole shot at a lower acquisition rate.

The typical k range accessible in the usual ALTAIR configuration is between $3 < k < 15$ cm^{-1}, with a high wavenumber resolution $\Delta k \sim 0.7$ cm^{-1}.

In order to reach shorter scales, the optical path of the ALTAIR bench has been slightly modified to double scattering angles and k range. Moreover, the second channel has been set to a fixed low value $k_2 = 8$ cm^{-1} to extend the first channel range as much as possible (taking into account the optical constraints): in this configuration, channel 1 wavenumber could be chosen between 5.5 and 26 cm^{-1}. The second channel was used as a scattering intensity reference. This modification divides the beam waist by 2, so that the k resolution was twice larger $\Delta k \sim 1.35$ cm^{-1}.

2.2. Localisation of the measurements

Scattering experiments are known to have a poor localization: this is the cost of high k resolution. Very small scattering angles (around 1 mrad) are required to reach the typical k range of 10 cm^{-1} using a CO_2 laser. The probing and reference beams are then almost overlaid along a vertical chord across a section of Tore Supra.

Wavenumbers of density fluctuations are mainly perpendicular to magnetic lines ($k_\perp >> k_\parallel$). This property combined with the high k resolution of the device allows to get a partial localisation along the vertical chord [7]. The q-profile is generally such that the pitch angle variation along a vertical chord yields a change in the fluctuations $k_\perp$ direction with respect to $\vec{u}_R$ (in the poloidal plane) and signal is coming from where the scattering wavevector $\vec{k}$ is locally perpendicular to magnetic field lines matching the Bragg condition $\vec{k} = \vec{k}_\perp$. The size of this region will then depend on the relative wavenumber resolution $\Delta k/k$. The spatial selectivity is evaluated knowing the pitch angle profile $\xi(y) = B_p/B_T$. Taking α the angle between the scattering wavevector $\vec{k}$ and $\vec{u}_R$, the spectral density of the scattered signal takes the form

$$S(\vec{k},\alpha) \propto \int < \delta n_k^2(y) > F_{\alpha,k}(y)dy \quad \text{with} \quad F_{\alpha,k}(y) = \exp\{-\frac{k^2}{\Delta k^2} 4\sin^2(\frac{\xi(y)-\alpha}{2})\}$$

$F_{\alpha,k}(y)$ expresses the localization effect, and $< \delta n_k^2(y) >$ is the local fluctuation spectral density. For a typical q-profile with q varying from 1 in the core to $q_a \sim 3$ at the edge, the pitch angle maximum is around $\pm 8^o$, while $\Delta k/k$ is of the order of 2 degrees for $k = 26$ cm^{-1}, around 8 degrees for $k = 8$ cm^{-1}. The selectivity function is ploted on figure 1b, which shows that only the lower edge contributes to the scattering signal when channels are set at the angle $\alpha_1 = \alpha_2 \sim -6°$. The scattering volume varies slightly on its upper and central part when k is changed from 8 to 26 cm^{-1}. As the fluctuation profile is strongly peaked near the edge, the contribution of these central zones remains very low; upper edge fluctuations will contribute slightly more at low k where selectivity is worse. The consequent variation of the total signal intensity, i.e. integrated along the whole chord, due to the change of selectivity does not exceed 20%.

In the experiments presented hereafter, plasma current was set to keep the edge safety factor at the value of $q_a = 3.3$ at the edge. The magnetic field line orientation profile along ALTAIR chord was thus kept similar for all experiments. The wavevector orientation was fixed in order to observe the plasma lower zone for both scattering channels ($r/a \sim 0.7$ to 1), and did not change during the experiments. In Ohmic of L mode plasmas with monotonic q-profile, the selectivity function is mainly sensitive to the maximum of pitch angle and thus to q_a; an error of $\Delta q_a = 0.5$ induces less than 15% of total intensity change.

2.3. Experimental procedure

The wavenumber k has been varied either from shot to shot, or continuously, at a rate of 1 cm^{-1} per second, depending on the possibility of exploring plasma parameters during the shot by varying the applied power P or from shot to shot by varying the magnetic field B or the gas. Both methods require reproducible plasmas since several identical shots are necessary to get a k-spectrum $S(\vec{k}) \equiv < i_{det}(\vec{k},t)^2 >_t \propto |n(\vec{k})|^2$ in the whole k range.

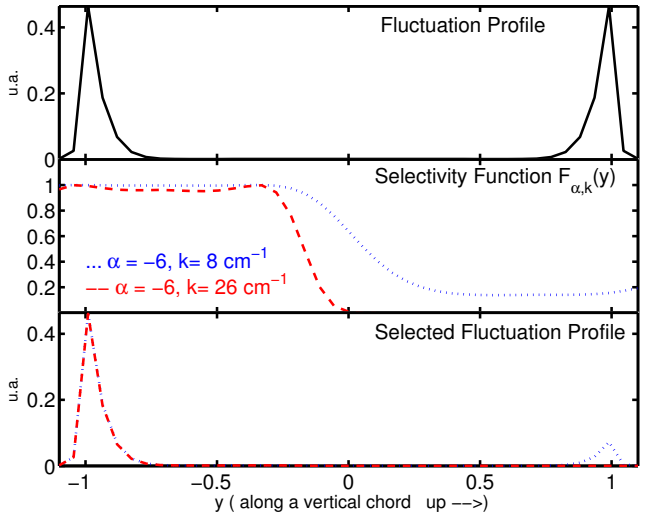

Figure 1. Instrumental selectivity $F_{\alpha,k}(y)$ along the vertical chord (b), showing how localisation varies from lower value (8 cm^{-1}, dots) to upper value of k (26 cm^{-1}, dashed). The fluctuation spectral density profile $< \delta n_k^2(y) >$ is shown (a). The contributing part of the fluctuation profile to the total scattered power are plotted in (c) for the upper and lower value of k.

Different typical lengths have been evaluated for each of the plasma conditions used in this study to be compared with the width or the characteristics of the wavenumber spectrum: the ion Larmor radius $\rho_i = \frac{v_{thi}}{\omega_{ci}} = \frac{\sqrt{m_i T_i}}{q_i B}$, the ion Larmor radius at T_e, $\rho_s = \frac{c_s}{\omega_{ci}} = \frac{\sqrt{m_i T_e}}{q_i B}$, the electron Larmor radius $\rho_e = \frac{v_{the}}{\omega_{ce}} = \frac{\sqrt{m_e T_e}}{q_e B}$, and the collisionless skin depth $\delta_s = \frac{c}{\omega_{pe}}$ the latter having been suggested as the relevant scale for the electron dynamics and electron thermal transport, with a scaling close to ETG one [15]. These parameters require the measurement of density and temperature profiles, since the scattering volume coincides with the outer part of the plasma $0.7 < r/a < 1$. The evaluation of the ion Larmor radius has the largest uncertainty: $T_i(r)$ is computed using the power balance code LOCO [40, 13] with constraints from the experimental data: central $T_i(0)$ value from the X-ray spectrometer, neutrons, global energetic content. The uncertainty is around 30% for the absolute value, but should be less for comparison of the different series.

3. Observation of a transition in the k-spectrum

3.1. Ohmic and L mode plasmas

In a first set of experiments, steps of ICRF heating power ($P = 0, 2, 4$ MW) were applied in deuterium plasmas, with $B = 3.2$ T, $I_p = 1.4$ MA, and the density kept nearly constant around $< n_e >= 3.5\ 10^{19}$ m^{-3}. Several identical shots (~ 10) were necessary to get the complete k-spectrum from 6 to 26 cm^{-1}.

The ion Larmor radius has been evaluated around $\rho_i \sim 0.9 \pm .3$ mm in $r/a = 0.8$ during the Ohmic phase [$\rho_s = 1. \pm .2$ mm]. The change in ρ_i is small between Ohmic and heating phases $\rho_i \sim 0.95 \pm .3$ mm, within the error bars: the profile analysis indicates in the scattering zone ($0.7 < r/a < 1$) a variation of the order of 5% with the applied power P=2 and 4 MW [$\rho_s = 1.05 \pm .2$ mm and $\rho_s = 1.1 \pm .2$ mm]. The Larmor radius for electrons is around $\rho_e = 20 \pm 5\,\mu$m (Ohmic phase), $\rho_e = 25 \pm 5\,\mu$m (P=2 and 4 MW). The skin depth, evaluated in $r/a = 0.8$, is around $\delta_s = 0.95 \pm .2$ mm during the Ohmic phase, and decreases slightly $\delta_s = 0.90 \pm .2$ mm when ICRF is applied.

The k spectrum obtained for the Ohmic phase is shown in figure 2(a), for the heating phase in figure 2(b). They both exhibit a transition around k_c = 14 - 15 cm^{-1}. This corresponds to $k_c\rho_i \sim 1.2 - 1.5$; this value is indicative since ρ_i varies by a factor of 2 in the scattering zone at the edge $1 < k_c\rho_i < 2$. The skin depth value δ_s is also found to be close to the Larmor radius, and should also be considered though its variation is opposite.

The lower k part of the spectrum is similar to former results obtained with ALTAIR [7]. The power spectrum was observed to be constant up to 4 to 6 cm^{-1}, decreasing then as $k^{-3\pm.5}$ in the wavenumber range up to 14 cm^{-1}. The dashed line on figure 2, obtained by fitting the lowest k data up to the transition, has been prolonged on the whole range to better show the transition. It indicates a spectral exponent of -3.5±.5 slightly larger than the one obtained with the usual configuration, that may be explained by the worse k resolution, (Δk is twice larger for this configuration) through an integration effect over a wider k domain. These results are also similar with observations from the cross polarization diagnostic on Tore Supra [36], indicating a spectral index of -3, and other tokamaks mentioned in the introduction.

Above 15 cm^{-1}, the power spectrum falls off much faster, typically with a power law, $S(k) \sim k^{-6.5\pm.5}$, determined by fitting the data in the wavenumber range above the transition. This is a large and significant decrease of the fluctuation level: nearly one order of magnitude between the expected value from the usual power law, and the actual one, at the largest k (as it has been shown in paragraph 2.2, the instrumental selectivity variation with k could not explain such a variation). This fast decrease is observed in the different plasma conditions: Ohmic, $P = 2, 4$ MW. A faster decrease is observed at larger heating power. Though the increase of the scaling exponent is within the error bar, it is significant since systematic: a similar observation has been made previously in L mode regime showing an larger increase of the larger scales with the applied power [43].

A change in the wavenumber spectrum power law is expected in several theories. It is characteristic of the 2D turbulence, and as mentioned in the introduction, usually invoked for explaining the wavenumber shape at small to medium k. The

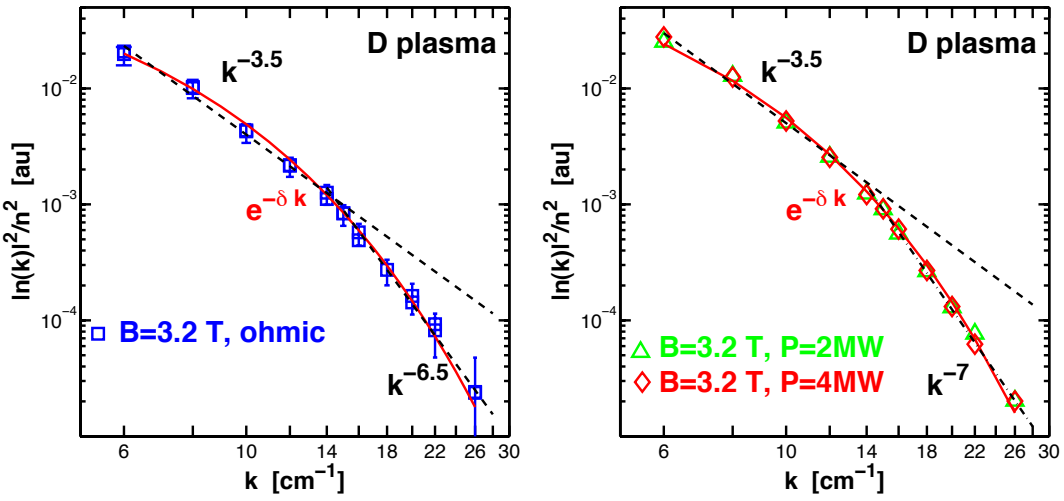

Figure 2. k spectrum of the density fluctuations $|n(\vec{k})|^2$ (normalised to the squared density) as a function of k (logarithmic scales). 3 series are compared at $B = 3.2$ T, Ohmic phase (a, squares), and L mode (b) at 2 additional heating power $P = 2$ MW (triangles) and 4 MW (diamonds). The power laws are obtained by fitting the data on either side of the transition (dashed lines), and prolonged on the whole k range. The plain line is the result of fitting the data with an exponential function $e^{-\delta k}$

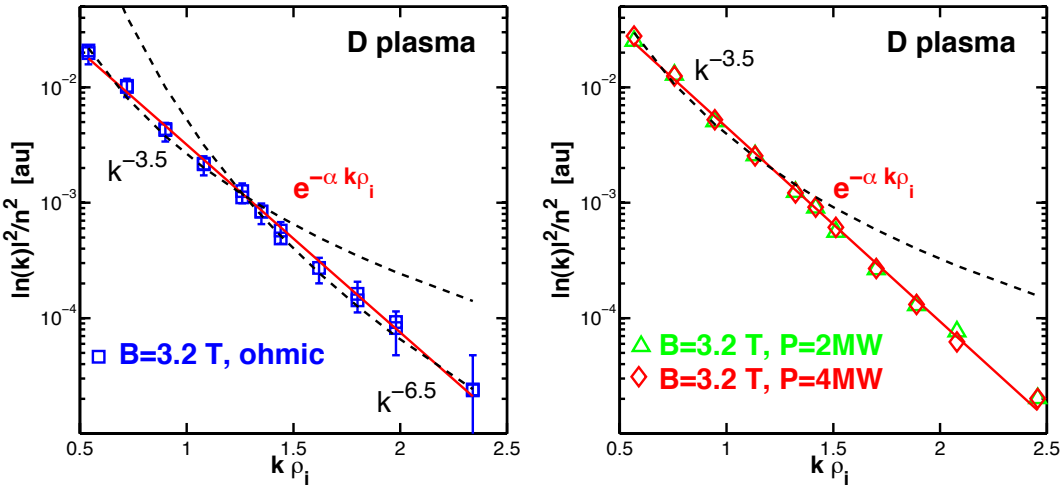

Figure 3. k spectrum of the density fluctuations $|n(\vec{k})|^2$ (normalised to the squared density) as a function of $k\rho_i$ (semilogarithmic scale). Same legend as in figure 2. The plain line is the result of fitting the data with an exponential function $e^{-\alpha k\rho_i}$, with $\alpha = 4 \pm .1$.

observed slopes are here very different: as previously shown, a spectral exponent around -4 is expected in the direct enstrophy cascade range, above the production scale, around $-8/3$ in the inverse cascade range. The fact that the exponents depend on plasma conditions is also not consistent with a fondamental assumption yielding these power laws: the existence of an inertial range, where no energy is injected nor

dissipated, and the energy transfer rate between scales does not depend on k nor on the system characterisitics. The transition should be expected around the energy injection scale, that is $k\rho_i \sim> 1$ from our results, though the most unstable modes are generally expected at much smaller wavenumber (typically $k\rho_i \sim 0.3$).

Finite Larmor radius effects should also yield a transition around $k\rho_i \sim 1$ [44, 4]; however the shape of the observed wavenumber spectrum is not described by these theories.

However the observation of a transition between two different ranges with different spectral exponents indicates that a characteristic length must be taken into account, breaking in this range the assumption of self-similarity and inertial range. Another way to represent the k spectrum clearly exhibits this characteristic length: the plain line on figure 2 (a,b) is the best fit of the spectrum with an exponential law of the form $e^{-\delta k}$. The k spectra are redrawn in figure 3 (a,b) on a semi-logarithmic scale as a function of $k\rho_i$ to better show the two representations; the power laws on either side of the transition are plotted in dashed lines, and prolonged over the whole range, the exponential law $e^{-\alpha k\rho_i}$, with $\alpha = 4$, is plotted in plain line. These two representations fit well the data, with a standard deviation slightly smaller (30%) for the exponential case. Yet theoretical implications are different: these spectral indexes and transition location remain to be explained within the statistical description of turbulence in the first case; though not expected in any classical theory, the exponential shape could be the signature of a more continuous length effect, for example due to damping processes or finite Larmor radius effect.

The spectrum of linear growth rates has been computed with the linear electrostatic gyro-kinetic code Kinezero [41] for these plasma conditions: ITG, TEM and ETG modes are unstable at the plasma periphery, with a dominant part of TEM. The largest growth rate ($\sim 10^5$ s^{-1}) is reached for $k\rho_i \sim 5$ to 10 (corresponding to $k\rho_e \sim 0.10$ to 0.20). Associated fluctuations should then be detected in our range of experiment ($k\rho_i$ up to 3), possibly rising the fluctuation amplitude in the range of unstable modes wavenumbers, even if the maximum is not reached. Our observations do not exhibit an increase of the level of fluctuation in this range and conversely show a fast decrease. We cannot though fully exclude the existence of ETG modes: the level of fluctuations associated with ETG may also increase in the domain of very high frequencies (> 2 MHz) or very high k values ($k\rho_i > 3$), not accessible with the present device. Experimental conditions may also not be optimum for the onset of these modes. Other observations should be done in optimized conditions for having a high predicted level of ETG, that is with a steep electron temperature gradient: on Tore Supra this could be done using fast wave ion cyclotron frequency heating, and these experiments have demonstrated a temperature gradient threshold and scaling consistent with expectations from ETG [42].

To address the question of a possible link of the transition with ρ_i, a larger

range on ρ_i was necessary and the magnetic field was then varied, which can be done on a large range on Tore Supra.

3.2. Magnetic field B scan in Ohmic plasma

Series of Ohmic helium discharges were performed with different toroidal magnetic fields: $B = 1.8$, 2.8 and 3.8 T. I_p is changed to keep q_a constant: 0.7 MA, 1 MA, 1.4 MA. The average density is around 1.6x10^{19} m^{-3}, 2.1x10^{19} m^{-3}, 2.8x10^{19} m^{-3} respectively.

The typical time sequence is plotted on figure 4. Making use of the motorized scattering angle, the wavenumber k of channel 1 was varied continuously in the plateau phase of the shot. The fluctuations RMS value of channel 1, whose k was varied from 9.5 to 15 cm^{-1} in that shot, is shown on figure 4(b). Replotted versus k it provides the expected wavenumber spectrum. The wavenumber of channel 2 is fixed $k_2 = 8$ cm^{-1}. The uncertainty on k_1 value is ± 1 cm^{-1} due to uncertainty on the motor position. Fast acquisitions were recorded (at times marked by the vertical bars), for a better estimate of $S(k)$ at large k, where signal to noise ratio is low. 5 such identical shots are necessary for completing the wavenumber spectrum on the whole range.

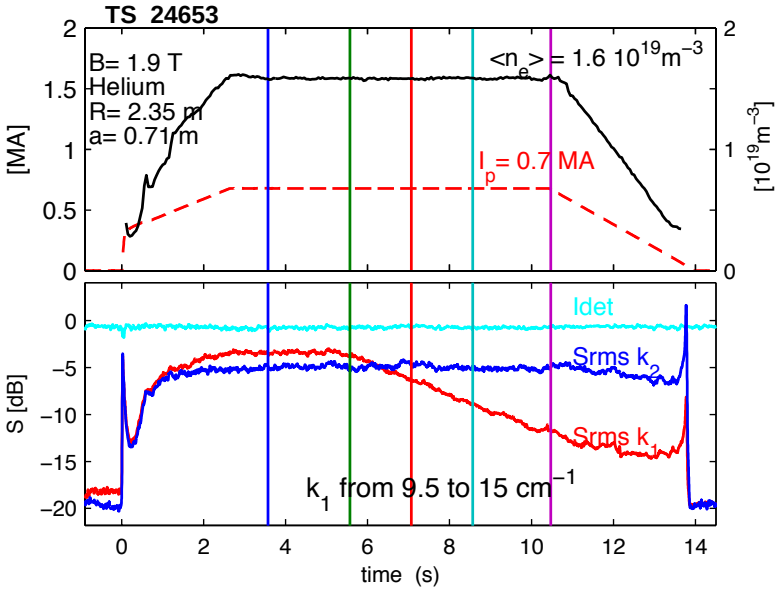

Figure 4. Time evolution of the density and plasma current. (b) Time evolution of the RMS value of the scattered signal: channel 1, k varies from $t \sim 5s$; channel 2 k is fixed at 8 cm^{-1}.

The table below summarizes the values of $\rho_{i,s,e}$ and δ_s at $r/a \sim .8$ for the different magnetic fields. The change in ρ_i is around 30% while doubling the magnetic field: the change of the temperature T partially compensates B variation due to the change of I_p.

Table 1. Larmor radius for ions and electrons, skin depth, evaluated in $r/a = 0.8$ for Ohmic helium series.

	ρ_i (mm)	ρ_s (mm)	ρ_e (μm)	δ_s (mm)
He, B=3.8 T	0.75 ±.5	0.9±.2	24 ±5	1.1±.2
He, B=2.8 T	1 ±.5	1.1 ±.2	30 ±5	1.3 ±.2
He, B=1.8 T	1.05 ±.5	1.25 ±.2	35 ±5	1.5 ±.2

The wavenumber spectrum $S(k)$ is shown on figure 5(a) for these He series (for seak of clarity, we only plot the data for extreme values of B). It exhibits a transition which changes clearly from high magnetic field (around 16 cm^{-1} for 3.8 T), to low magnetic field (12 cm^{-1}, for 1.8 T). This shift of the transition is compatible with the change in ρ_i. It corresponds to $k_c\rho_i \sim 1.2 - 1.5$, as in section 2.

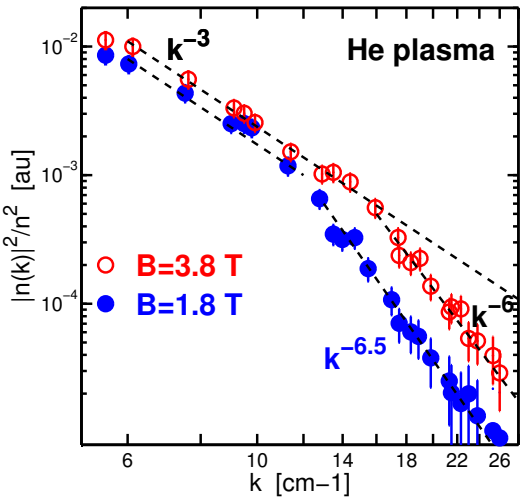

Figure 5. k spectrum of the density fluctuations $|n(\vec{k})|^2$ (normalised to the squared density) as a function of k (logarithmic scales). Ohmic discharges in He are compared with $B = 3.8$ T (open circles) and $B = 1.8$ T (closed circles).

The shape of the k spectrum is similar the one obtained in the conditions of section 2. Above the transition, the k-spectrum follows a power law, $S(k) \sim k^{-6.\pm.5}$, determined by fitting the data in the wavenumber range above the transition. The spectral index also varies slightly with the ion Larmor radius, as the intensity decreases faster for smaller toroidal magnetic field. The k spectra are redrawn in figure 5 on a semi-logarithmic scale, as a function of k in (a) and as a function of $k\rho_i$ in (b). The data are fitted by an exponential functions $e^{-\alpha k\rho_i}$ plotted in plain line: the same factor $\alpha = 4$ is found for low and high ρ_i.

The same dependence of the transition location with the gyroradius is obtained in Deuterium when changing the magnetic field (3.8 to 2.5T). However changing the gas from He to D has not shown a shift of the transition k_c: at given magnetic

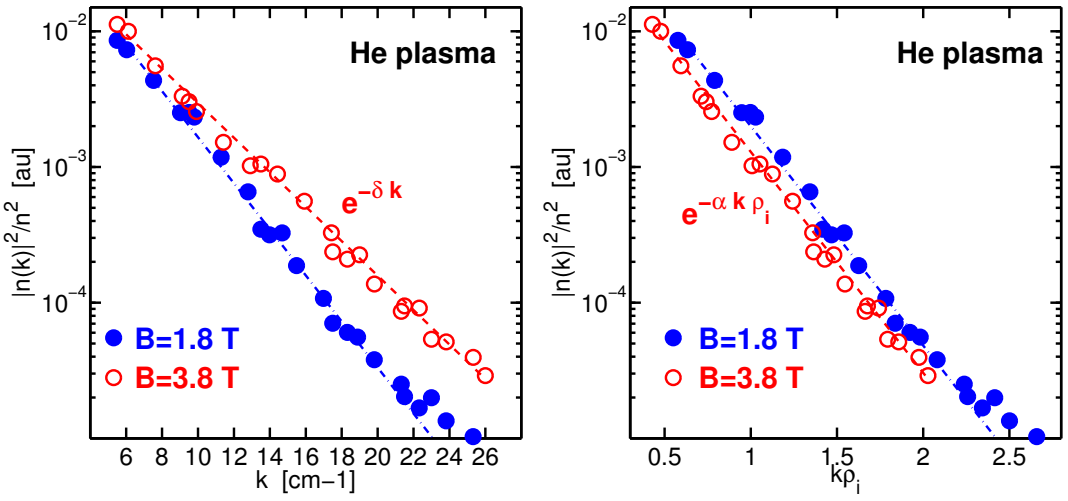

Figure 6. k spectrum of the density fluctuations $|n(\vec{k})|^2$ (normalised to the squared density) as a function of k (a) and as a function of $k\rho_i$ (semilogarithmic scale). Same legend as figure 5.

field, it is comparable in He and D series. However, the isotopic effect is hidden by dilution effects in these Ohmic plasmas, and very comparable values of ρ_i are indeed found in both series.

4. Fluctuation level scaling with the ion gyroradius ρ_i

These different plasma conditions made it possible to also compare the level of fluctuation with what is expected from the mixing length theory. The latter predicts that the relative fluctuation level scales as $1/(< k_\perp > L_n)$, where L_n is the density gradient length [3], that is $\delta n/n \equiv \rho_i/L_n$ (gyro-Bohm). The density fluctuation k spectrum is thus normalized to the squared density and ρ_i^2 (the gradient length is similar $L_n \sim 0.4$ m for both experiments) and plotted as a function of $k\rho_i$ in figure 7 (same data as figure 5). It shows a good matching of the data between the two extreme values of ρ_i. This agreement is also observed for all the series. The global confinement time varies from 0.15 s (B= 1.8 T) to 0.26 s (B=3.8 T) and follows rather a gyroBohm scaling. This consistency with a gyro-Bohm scaling of the fluctuations has already been obtained on Tore Supra [45, 22] and other tokamak experiments [21, 9].

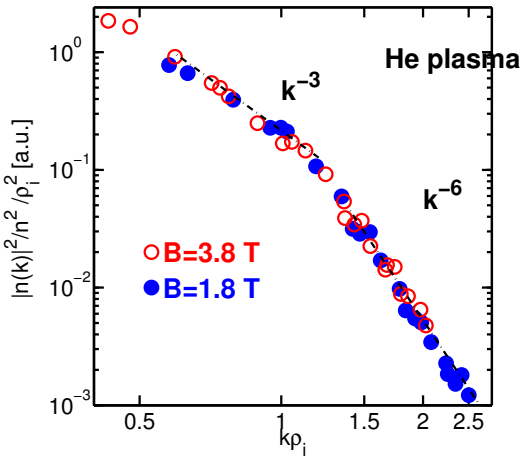

Figure 7. k spectrum of density fluctuations $|n(\vec{k})|^2$ (normalised to the squared density) divided by (ρ_i^2) as a function of $k\rho_i$ for the He series.

5. Correlation time scaling with the transit time L/c_s

The correlation time of the signal modulus is plotted in figure 8 (a) as a function of k: it varies from a few μs at small k to a fraction of μs at higher k. This correlation time should be linked with the typical transit time $\tau_T \equiv a/c_s$. Correlations times have thus been normalized to $\tau_c/(a/c_s)$ and plotted as a function of $k\rho_i$ on figure 8 (b). The matching between the two series in He at low and high ρ_i is rather good. This scaling of the turbulence correlation time with a/c_s has already been observed in other tokamak experiments [9]. Together with the scaling of turbulence scale length with ρ_i, it supports the picture of turbulence characteristics leading to a gyroBohm scaling of confinement.

This correlation time is related to the lifetime of the turbulent structure, and should behave as the eddy turn-over time. Our observations show that τ_c decreases as k^{-1}. This typical dependence was already observed in earlier experiments with ALTAIR [47] and is also observed in fluid experiments [37]. In 3D fluid turbulence, the eddy turn-over time should scale $\tau_c \equiv k^{-2/3}$ resulting of Kolmogorov power law [24, 25]. Our observations are more consistent with a transit time in hydromagnetic turbulence [48] or decorrelation time of the structures driven by the sweeping of these structures by the largest and most energetic structures [49]: this leads to a typical time $\tau_c = 1/\bar{u}k$ where $\bar{u}$ does not depend on k.

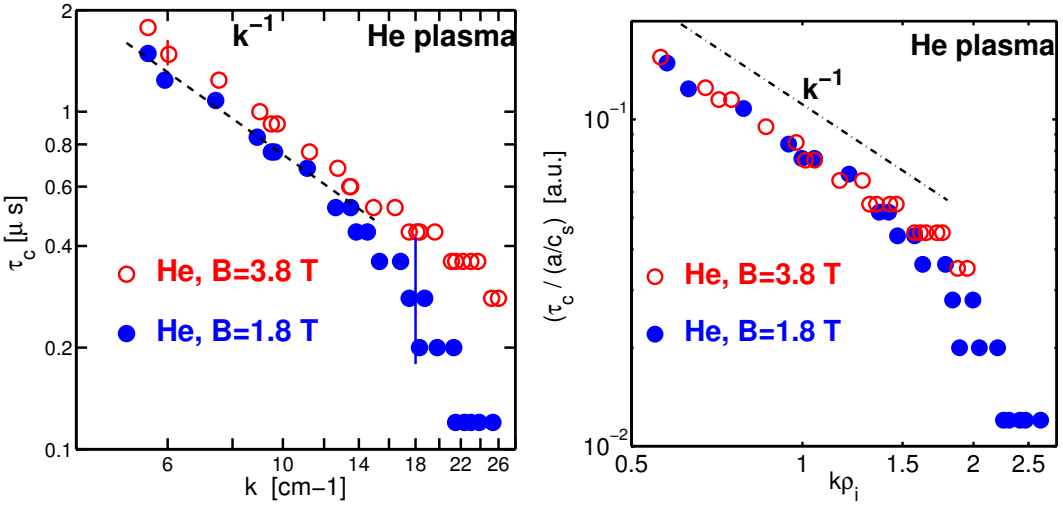

Figure 8. Signal modulus correlation time as a function of the wavenumber spectrum (a) and normalised to (a/c_s) as a function of $k\rho_i$.

6. Conclusion

In this paper we relate an unexpected behaviour of fluctations at high k. The fluctuation level turns out to decrease much faster for scales smaller than ρ_i, typically with a power law $S(k) \equiv k^{-6}$, than usual observations $S(k) \equiv k^{-3}$. The transition is observed for $1 < k\rho_i < 2$. This transition indicates that a characteristic scale should be involved to describe the fluctuation non linear dynamics in this range. This could be the signature in this wavenumber range of a breakdown of 2D description of turbulence, through other forcing process or a change in the nature of turbulence. This could be also the sign of a wider scale length effect (finite Larmor radius effect, damping) since our data are also well fitted by an exponential law $e^{-4k\rho_i}$ in the whole range and for all the conditions studied.

The results at high and low ρ_i exhibit a good matching with predictions from a gyro-Bohm scaling of the turbulence: the typical scale length of turbulence scales

with the ion Larmor radius, the typical time scales with a/c_s; the turbulence level also scales with ρ_i, according to the mixing length rule. Yet the confinement scaling with $\nu*$ and β is still being debated, and dimensionless studies of turbulence should be extended to these parameters.

References

[1] J.D. Callen, et al., *Physics Today*, 34, (1992). J.D. Callen. *Phys. Fluids B*, **4**, 2142 (1992).
[2] J.W. Connor. *Plasma Phys. Control. Fusion*, **35**, B293–B305 (1993).
[3] X. Garbet, *Plasma Phys. Control. Fusion*, **43**, A251 (2001) *and this conf.*
[4] W. Horton, *Rev. Mod. Phys.*, **71**, 735 (1999).
[5] Ritz C P, D.L. Brower, Rhodes T L, Bengston R D, Levinson S J, Luhmann N C Jr, Peebles W A and Powers E J, *Nucl. Fusion* **27**, 1125 (1987).
[6] Paul S F, Bretz N, Durst R D, Fonck R J, Kim Y J, Mazzucato E and Nazikian R, *Phys. Fluids B*, **4** 2922 (1992).
[7] Devynck P, Garbet X, Laviron C, Payan J, Saha S K, Gervais F, Hennequin P, Quemeneur A and Truc A, *Plasma Phys. Control Fusion*, **35**, 63 (1993).
[8] Fonck R J, Cosby G, Durst R D, Paul S F, Bretz N, Scott S, Synakowski E and Taylor G, *Phys. Rev. Lett.*, **70**, 3736 (1993).
[9] G.R. McKee, C.C Petty, R.E. Waltz, C. Fenzi, R.J. Fonck, J.E. Kinsey, T.C. Luce, *et al.*, *Nucl. Fusion*, **41**, 1253 (2001).
[10] Mazzucato, E. et al.,*Phys. Rev. Lett.* **77**, 3145 (1996).
[11] C. L. Rettig, W.A. Peebles, E.J. Doyle, K. H. Burrell, C. Greenfield, G.M. Staebler, B.W. Rice. *Phys Plasmas*, **4**, 4009 (1997)
[12] B. W. Stallard et al.,*Phys Plasmas*, **6**, 1978 (1999)
[13] G.T Hoang et al., *Nucl. Fusion*, **38**, 117 (1998)
[14] G.T Hoang et al., *Phys. Rev. Lett.*, **87**, 125001 (2001)
[15] F. Jenko, W. Dorland, M. Kotschenreuter and B.N. Rogers,*Phys Plasmas*, **7**, 1904 (2000)
[16] F. Jenko and W. Dorland,*Phys. Rev. Lett.*, **89**, 225001-1 (2002)
[17] F. B. Labit and M. Ottaviani,*Phys Plasmas*, **10**, 13 (2003)
[18] J.W. Connor et al, *Nucl. Fusion*, **17**, 1047 (1977).
[19] J G Cordey, B Balet, D Campbell, C D Challis, J P Christiansen, C Gormezano, C Gowers, D Muir, E Righi, G R Saibene, P M Stubberfield and K Thomsen, *Plasma Phys. Control Fusion*, **38**, A67 (1996).
[20] J. Weiland, *Collective Modes in Inhomogeneous Plasmas*, IOP (2000).
[21] T. Crowley, E. Mazzucato, *Nucl. Fusion*, **25**, 507 (1985).
[22] Zou, X.L., et al., *In Proc. of 24th Eur. Conf. on Control. Fusion and Plasma Phys, 1997*, Vol. III, (1998).
[23] T. L. Rhodes, *et al.In Proc. of 27th Eur. Conf. on Control. Fusion and Plasma Phys., Budapest, 2000.*
[24] U. Frisch, *Turbulence: The legacy of Kolmogorov*, Cambridge University Press (1996)
[25] M. Lesieur, *Turbulence in Fluids*, Kluwer Academic Publishers Ed. (1997).
[26] R. Kraichnan, *Phys. Fluids*, **10**, 1417 (1967).
[27] D. Fyfe and D. Montgomery, *Phys Fluids*, **22**, 246 (1979).
[28] A. Hasegawa and M. Wakatani, *Phys. Rev. Lett.*, **50**, 682 (1983).
[29] F. Jenko and B. Scott, *Phys Plasmas*, **6**, 2418 (1999).
[30] Mazzucato, E., *Phys. Rev. Lett.* , **36**, 792 (1976). E. Mazzucato, *Phys. Fluids*, **21**, 1063 (1978).
[31] Surko, C. M., and R. E. Slusher, *Phys. Rev. Lett.*, **36**, 1747 (1976).
[32] A. Semet, A. Mase, W.A. Peebles, N.C. Luhmann, S Zweben, *Phys. Rev. Lett.*, **45**, 445 (1980).
[33] E. Mazzucato, *Phys. Rev. Lett.*, **48**, 1828 (1982).

[34] D.L. Brower, W.A. Peebles, N.C. Luhmann, Jr., R. Savage, *Phys. Rev. Lett.*, **54**, 689 (1985).
[35] D.L. Brower, W.A. Peebles, N.C. Luhmann, Jr., *Nucl. Fusion*, **27**, 2055 (1987).
[36] Zou, X.L., et al., *In Proc. of 26th Eur. Conf. on Control. Fusion and Plasma Phys., Maastricht, 1999*, Vol. 23J, 1041 (1999).
[37] C. Honoré and D. Grésillon. *Journal of Fluid Mechanics*, **411**, 187, (2000).
[38] A. Truc, A. Quémeneur, P. Hennequin, D. Grésillon, F. Gervais, C. Laviron, J. Olivain, S.K. Saha, and P. Devynck. *Rev. Sci. Instrum.*, **63**, 3716 (1992).
[39] C. Honoré, R. Sabot, P. Hennequin, *et al.*, In *Proc. of 25th Eur. Conf. of Plasma Phys. and Control. Fusion*, Prague, 1998. vol 22C, 647.
[40] Harris, G.R., Capes, H., Garbet, X., *Nucl. Fusion*, **32**, 1967 (1992).
[41] C. Bourdelle, *et al.*, *Nucl. Fusion*, **42**, 892 (2002).
[42] G. T. Hoang, W. Horton, C. Bourdelle, B. Hu, X. Garbet, and M. Ottaviani. *Phys Plasmas*, **10**, 405 (2003).
[43] P. Devynck, F. Clairet, X.L. Zou, X. Garbet, L. Colas, P. Moreau, C. Laviron, G.T. Hoang, A. Truc, P. Hennequin, F. Gervais, A. Quemeneur. *Plasma Phys. and Controlled Fusion*, **39**, 9, 1355 (1997).
[44] Hasegawa A., and Mima K., *Phys. Rev. Lett.*, **39**, 205 (1977).
[45] C. Laviron, & al *In Proc. 16th IAEA Fusion Energy Conf., Montréal, Oct. 1996*, IAEA-CN-64/A6-3, IAEA Vienna, Vol. 1, 535 (1997).
[46] Zou, X.L., et al., *In Proc. of 23th Eur. Conf. on Control. Fusion and Plasma Phys, 1996*, Vol. III, (1997).
[47] C. Honoré, P. Hennequin, *et al.*, In *Proc. of 27th Eur. Conf. of Plasma Phys. and Control. Fusion*, Budapest, 2000. vol 24B, 1036.
[48] R. Kraichnan, *Phys. Fluids*, **8**, 1385 (1965).
[49] R. Kraichnan, *J. Fluid Mech.*, **5**, 497 (1958).